

ZERO-SHOT INVERSION PROCESS FOR IMAGE ATTRIBUTE EDITING WITH DIFFUSION MODELS

Zhanbo Feng^{*1}, Zenan Ling^{*†2}, Ci Gong², Feng Zhou³, Jie Li¹ & Robert C. Qiu²

¹ Department of Computer Science and Engineering, Shanghai Jiao Tong University

² EIC, Huazhong University of Science and Technology

³ Center for Applied Statistics and School of Statistics, Renmin University of China

ABSTRACT

Denosing diffusion models have shown outstanding performance in image editing. Existing works tend to use either image-guided methods, which provide a visual reference but lack control over semantic coherence, or text-guided methods, which ensure faithfulness to text guidance but lack visual quality. To address the problem, we propose the Zero-shot Inversion Process (ZIP), a framework that injects a fusion of generated visual reference and text guidance into the semantic latent space of a *frozen* pre-trained diffusion model. Only using a tiny neural network, the proposed ZIP produces diverse content and attributes under the intuitive control of the text prompt. Moreover, ZIP shows remarkable robustness for both in-domain and out-of-domain attribute manipulation on real images. We perform detailed experiments on various benchmark datasets. Compared to state-of-the-art methods, ZIP produces images of equivalent quality while providing a realistic editing effect.

1 INTRODUCTION

Manipulating real-world images with natural language has long been a challenge in image processing. Recently, denosing diffusion models (DDMs) have shown substantial success in text-to-image tasks, such as Imagen (Saharia et al., 2022), Dall-E (Ramesh et al., 2021), and Stable Diffusion (Rombach et al., 2022). These text-to-image models produce diverse, highly coherent, and realistic images that align well with text prompts. However, attribute manipulation on real images is still a challenging problem. In this paper, we aim to utilize these novel foundational models to manipulate real images in a controllable and semantically coherent manner.

Figure 1 briefly illustrate currently popular methodologies. On the one hand, much effort has been put into text-guided image editing. Along with the development of the Natural Language Processing (NLP) technique, e.g., Generative Pre-Training (GPT) (OpenAI, 2023; Brown et al., 2020), many previous works (Bao et al., 2023; Hertz et al., 2022) develop image-editing techniques with the guidance of textual prompts. However, the importance of the visual reference is ignored in these methods. Though text-guided methods maintain faithfulness to the target semantic, it is difficult to learn fine-grained visual patterns from textual features in the absence of a visual prior. Using textual semantics alone lacks visual reference, resulting in sketchy semantic manipulation. Especially if the desired semantic is out of the domain, text-guided editing fails.

On the other hand, image-guided methods attract a large amount of attention. Image-guided editing can easily make style transfer (Choi et al., 2021) and item replacement (Jia et al., 2023). With visual reference, generators can directly insert ready-made visual patterns into images. However, image-guided approaches lack intuitive control over semantic coherence, and it is ambiguous to specify which attribute to refer from the reference image.

In recent times, there has been a growing interest in the field of real image editing. Prompt2Prompt (Hertz et al., 2022) has shed light on the potential of cross-attention layers for

^{*} Equal contribution.

[†] Corresponding author. Email: lingzenan@hust.edu.cn

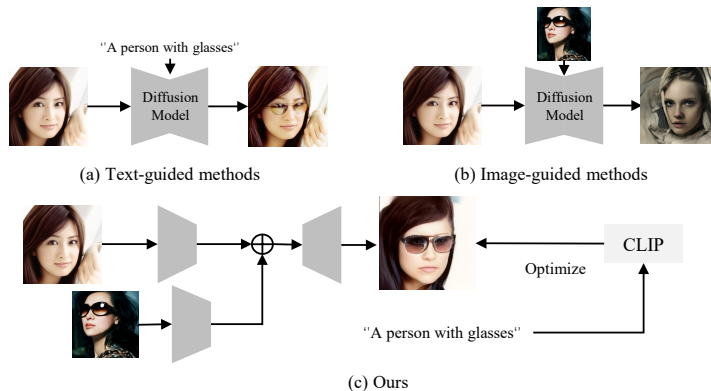


Figure 1: **Editing methods for denoising diffusion models.** (a) Text-guided methods lacks a predefined style of the attribute, where the glasses are generated by models. (b) Image-guided methods suffer ambiguity and distorted results. (c) Our method achieves specific, controllable and high-quality manipulation, where the style of glasses is in accordance with the reference image.

semantic editing in image generation. Following this, InstructPix2Pix (Brooks et al., 2023) and Null-text Inversion (Mokady et al., 2022) employed the same principle for semantic editing of real images. However, one limitation of these approaches is their inability to precisely control specific attributes during the editing process. For instance, as demonstrated in Figure 1(a), the glasses added by Null-text Inversion lacks a predefined style, making it challenging to confirm the exact appearance of the added glasses in advance. The visual prompt can serve to accurately delineate the desired attributes. Jia et al. (2023) embeds specified items into the target image by encoding a reference image. VISII (Nguyen et al., 2023) amalgamates both textual and visual prompts to learn a style transfer from example pairs, representing the “before” and “after” images of an edit. Nevertheless, as shown in Figure 1(b), when a reference image is employed for attribute editing of real images, the final rendition is effected by the reference image, which causes image distortion.

In this paper, we propose Zero-shot Inversion Process (ZIP) that injects a fusion of visual reference and text guidance into the semantic latent space of a *frozen* pre-trained diffusion model. As illustrated in Figure 1(c), our method takes advantage of the text guidance to provide intuitive control over the semantic coherence. Meanwhile, our methods refine the alignment of the text feature and the semantic latent space of the diffusion model by incorporating a visual reference. The incorporated reference image can be generated with a foundational text-to-image model. Thus, our method is zero-shot and avoids the bias of manual selection. To the best of our knowledge, it is the first attempt to integrate text guidance and image guidance in zero-shot image editing. Our method only needs to train an attribute encoder, a tiny neural network, without fine-tuning the pre-trained model. For both in-domain and out-of-domain attribute editing tasks, our method preserves faithfulness to text guidance while maintaining visual quality. Extensive experiments demonstrate that our method is generally applicable to various benchmark datasets (CelebA-HQ, LSUN-church, and LSUN-bedroom).

2 RELATED WORK

Text-to-Image Synthesis: Since the success of large language models, text prompts are widely used in image editing. Benefiting from the semantic information of text, Stable Diffusion (Rombach et al., 2022) makes a powerful and flexible generator with the condition of the text. Diffusionclip (Kim et al., 2022) shows that a textual prompt allows DDMs to edit the images in a semantic latent space. Asyrp (Kwon et al., 2022) reveals that diffusion models already have a semantic latent space. Imagen Editor (Wang et al., 2022) uses masks as input to point out the area of edit in the image, which can gather up the semantic information into the target. Though these works show a significant process in the editing of some attributes, only by text prompt, they just can generate ordinary attributes such as colors or common shapes in the image. To generate new visual features, such as glasses and other decorations in the images, the visual information should be taken into account.

Image-to-Image Synthesis: In contrast, image-guided approaches use the reference image as a condition to generate corresponding images. On the one hand, the features from the reference image

are used to adjust the target image. There are many typical tasks such as style transfer (Choi et al., 2021; Meng et al., 2021) and inpainting (Lugmayr et al., 2022), where the reference image is viewed as an auxiliary feature. SDEdit (Meng et al., 2021) uses the stroke-based images to generate faithful images with the original images. On the other hand, the reference image is directly inserted into the target image. Jia et al. (2023) makes remarkable performance by using the reference image for personalized syntheses, such as the replacement of the items. Mystyle (Nitzan et al., 2022) adopts a pre-trained StyleGAN for personalized face generation by using the images of the generic face prior. However, due to the ambiguity of the attribute choice in one image, image-guided approaches often make distorted images or incorrect manipulation. By using the text prompt, our ZIP circumvents this drawback with the alignment of visual features and semantic information from text.

Attribute Editing Many previous works (Kwon et al., 2022; Wallace et al., 2022; Daras and Dimakis, 2022) have focused on image editing based on large-scale generative models. On the one hand, these models mainly focus on editing DDM-generated images rather than real images. By adding, replacing, or modifying corresponding features, Prompt2prompt (Hertz et al., 2022) can change the items of a DDM-generated image. However, it is difficult to learn textual features corresponding to the real image. On the other hand, some models can only achieve sketchy editing for real images. For example, the background replacement is made in Direct Inversion (Elarabawy et al., 2022). The replacement of items in the real images is achieved in Jia et al. (2023). Some in-domain attributes, such as the age, gender, and expression of humans, are modified by Asyrp (Kwon et al., 2022). However, these models are incomplete for the attributes which need both visual and semantic information such as wearing glasses.

3 PRELIMINARY

In this section, we provide a concise overview of the foundational knowledge of the diffusion model and the Contrastive Language-Image Pre-Training (CLIP) model. The diffusion model is employed for the generation of visual prompts, facilitating the editing of real images. Subsequently, CLIP is utilized to adjust the images in accordance with the textual prompt.

3.1 DIFFUSION MODEL

Denosing diffusion models (DDMs) produce more realistic samples than deep generative models before, such as GANs (Karras et al., 2020). A typical DDM includes two stages: the forward process to add Gauss noise to the original data and the reverse process to denoise samples until an image. Denosing Diffusion Probabilistic Model (DDPM) (Ho et al., 2020), starting from white noise, progressively denoises it into an image. Denosing Diffusion Implicit Models (DDIM) (Song et al., 2020a) reduce the number of iterations by taking generated results of different stages into the condition of generation.

The forward process diffuses the original data x_0 with Gaussian noise, indexed by a real vector $\sigma \in \mathbb{R}_{\geq 0}^T$:

$$q_\sigma(x_{1:T}|x_0) := q_\sigma(x_T|x_0) \prod_{t=2}^T q_\sigma(x_{t-1}|x_t, x_0), \quad (1)$$

where $q_\sigma(x_T|x_0) = \mathcal{N}(\sqrt{\alpha_T}, (1 - \alpha_T)\mathbf{I})$. The corresponding reverse process is

$$x_{t-1} = \sqrt{\alpha_{t-1}/\alpha_t} (x_t - \sqrt{1 - \alpha_t}\epsilon_\theta(x_t, t)) + \sqrt{1 - \alpha_{t-1} - \sigma_t^2} \cdot \epsilon_\theta(x_t, t) + \sigma_t \epsilon_t, \quad (2)$$

where $\epsilon_t \sim \mathcal{N}(\mathbf{0}, \mathbf{I})$ is standard Gaussian noise, α_t is the parameter based on the forward process, $\sigma_t = \eta\sqrt{(1 - \alpha_{t-1})/(1 - \alpha_t)}\sqrt{1 - \alpha_t/\alpha_{t-1}}$, and $\epsilon_\theta(x_t, t)$ is a neural network to predict the noise in x_t . In this paper, we use a U-Net backbone which is introduced in the supplementary material. When $\eta = 1$ for all t , the process of Equation 2 becomes DDPM (Ho et al., 2020). As $\eta = 0$, it becomes DDIM and guarantees nearly perfect inversion (Song et al., 2020a).

3.2 CONTRASTIVE LANGUAGE-IMAGE PRE-TRAINING

Contrastive Language-Image Pre-Training (CLIP) (Radford et al., 2021) encapsulates generic and semantic information of image-text pairs. CLIP simultaneously learns an image encoder E_I and a

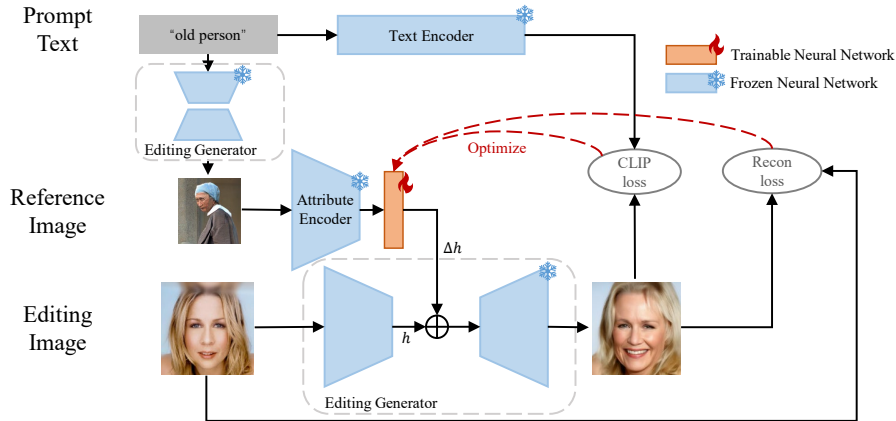


Figure 2: **The framework of ZIP.** A reference image, generated by the Visual Generator, is encoded into edited features denoted as Δh . These edited features are then integrated into the existing features h of the editing image. The textual prompt contributes semantic information for the manipulation process. To streamline computation, the parameters of both the Attribute Encoder and Editing Generator are shared.

text encoder E_T to indicate the similarity between images and texts. StyleGAN-NADA (Gal et al., 2022) produces images guided by a text prompt based on CLIP. Asyrp (Kwon et al., 2022) also uses the CLIP to fine tune the pre-trained diffusion model. Inspired by previous works, we adopt CLIP as guidance for the attribute modification:

$$\mathcal{L}_{\text{direction}}(i_{\text{out}}, t_{\text{target}}; i_{\text{edit}}, t_{\text{source}}) := 1 - \frac{\Delta I \cdot \Delta T}{\|\Delta I\| \|\Delta T\|}, \quad (3)$$

where $\Delta I = E_I(i_{\text{out}}) - E_I(i_{\text{edit}})$ and $\Delta T = E_T(t_{\text{target}}) - E_T(t_{\text{source}})$, for the generated image i_{out} , the editing image i_{edit} , the target prompt t_{target} , and the source prompt t_{source} .

4 METHOD

We present the Zero-shot Inversion Process (ZIP) as a method for attribute editing. The core framework of ZIP is outlined in Figure 2, where each constituent element of the framework is delineated. Subsequently, the principle of ZIP is elaborated in Section 4.1. Then, the optimization process and the associated loss function of ZIP are discussed in Section 4.2. Finally, we summarize the real image editing via ZIP in Section 4.3.

Given an image $i_{\text{edit}} \in \mathbb{R}^{m \times n}$ and an attribute t_{attr} , our primary objective is to modify the input image i_{edit} in accordance with the attribute t_{attr} . This endeavor results in the creation of an edited image, denoted as i_{out} . Initially, a textual prompt denoted as t is formulated based on the specific attribute t_{attr} , an example being the prompt "an old person" associated with the "old" attribute. Subsequently, the Visual Generator produces a reference image i_{ref} conditioned on the input t . In the third step, attribute features Δh are extracted from i_{ref} using the Attribute Encoder. Following this derivation, Δh is integrated into the latent space of the Editing image. The resultant latent representation $h + \Delta h$ forms the basis for generating the target image i_{out} through the Editing Generator.

As illustrated in Figure 2, our framework encompasses four primary components: Text Encoder, Visual Generator, Attribute Encoder, and Editing Generator. To obtain the visual attributes corresponding to the designated attribute, we utilize a text-image model as Visual Generator. Furthermore, when the attribute involves the addition of embellishments, such as the glasses, a reference image can be manually specified to ensure consistency of embellishments during editing. Both the textual prompt and the visual prompt, which are encoded by Text Encoder and Attribute Encoder respectively, are employed for editing in the Editing Generator. Detailed descriptions of these components are provided in Appendix B.

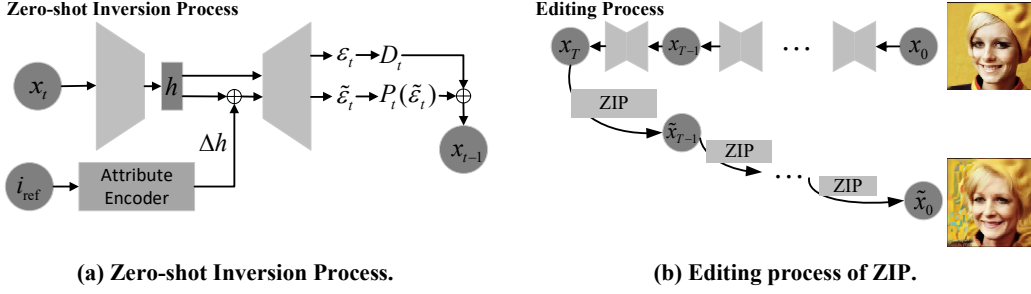


Figure 3: **Zero-shot Inversion Process.** (a) The one step from x_t to x_{t-1} in Zero-shot Inversion Process. (b) The inversion process and the forward editing process for a real image.

4.1 ZERO-SHOT INVERSION PROCESS

Figure 3 provides a thorough overview of the entire Zero-shot Inversion Process (ZIP). Figure 3(a) reveals its denoising process, where the feature Δh from the reference image i_{ref} is integrated into the original features h . Figure 3(b) illustrates the editing process in ZIP, where i_{edit} is reverted to noise x_T and subsequently restored to \tilde{x}_0 as i_{out} by ZIP.

As shown in Figure 3(a), the visual attributes extracted from the reference image i_{ref} are integrated into the editing image i_{edit} to amplify latent visual attributes that were hitherto unseen. For the generation of the reference image i_{ref} under the influence of the prompt condition t_{target} , we employ UniDiffuser (Bao et al., 2023). Subsequently, through the utilization of the Attribute Encoder, we extract the corresponding features $\Delta h = E_A(i_{\text{ref}})$.

To facilitate latent manipulation on the images x_0 generated from x_T , a straightforward approach could involve directly modifying the Attribute Encoder to minimize the loss outlined in Equation 3. However, adopting this approach might engender distorted images or erroneous manipulations, as observed in prior works (Choi et al., 2021; Mokady et al., 2022).

An alternative approach entails the modification of the noise ϵ_t^θ anticipated by the network during each sampling iteration. In brief, we can express the abridged version of Equation 2 as follows:

$$x_{t-1} = \underbrace{\sqrt{\alpha_{t-1}} \frac{1}{\sqrt{\alpha_t}} (x_t - \sqrt{1 - \alpha_t} \epsilon_\theta(x_t, t))}_{\text{predicted } x_0, P_t(\epsilon_\theta(x_t, t))} + \underbrace{\sqrt{1 - \alpha_{t-1} - \sigma_t^2} \cdot \epsilon_\theta(x_t, t)}_{\text{direction to } x_t, D_t(\epsilon_\theta(x_t, t))} + \sigma_t \epsilon_t. \quad (4)$$

Nonetheless, a direct alteration of the noise ϵ_θ in both P_t and D_t leads to mutual nullification, yielding an unchanged $p_\theta(x_{0:T})$. This phenomenon mirrors a form of destructive interference, as elucidated in Kwon et al. (2022, Theorem 1).

Hence, in order to circumvent the interference delineated in Equation 4, we resort to the utilization of an asymmetrical controllable reverse process within ZIP:

$$x_{t-1} = \sqrt{\alpha_{t-1}} P_t(\tilde{\epsilon}_\theta(x_t, t)) + D_t(\epsilon_\theta(x_t, t)) + \sigma_t \epsilon_t. \quad (5)$$

Here, $\tilde{\epsilon}_\theta(x_t, t)$ entails the adjustment of $\epsilon_\theta(x_t, t)$ grounded on the visual features Δh . This is achieved by introducing Δh into the original feature maps h_t derived from x_t .

4.2 OPTIMIZATION OF ZIP

Within the text-guided branch of ZIP, the text prompt t is harnessed to facilitate the optimization of the ZIP generation process, relying on the CLIP model. Given the absence of ground truth labels in editing tasks, training the model follows a distinct approach compared to conventional vision tasks. As a result, we employ the CLIP loss to fine-tune the network. Aligning with the methodology presented in Avrahami et al. (2022), we employ the directional CLIP loss outlined in Equation 3 as our loss function:

$$\mathcal{L} = \lambda_{\text{clip}} \mathcal{L}_{\text{direction}}(\tilde{P}_t, t_{\text{target}}; P_t, t_{\text{source}}) + \lambda_{\text{recon}} |x_{\text{out}}^t - x_{\text{edit}}^t|. \quad (6)$$

Algorithm 1 Zero-shot Inversion Process (ZIP)

Input: An editing image i_{edit} ; A text prompt t_{attr}
 Editing Generator ϵ_{θ} ; Visual Generator G_V ; Attribute Encoder E_A CLIP encoder ξ_{clip}
 Diffusion model timestep T ; ZIP timestep t_{zip}

Output: A target image i_{out}

- 1: Initialize t_{source} and t_{target} based on t_{attr} ▷ Get the textual prompt
- 2: Generate the reference image $i_{\text{ref}} = G_V(t_{\text{target}})$ ▷ Get the visual prompt
- 3: Encode $\Delta h = E_A(i_{\text{ref}})$
- 4: Get the noise image x_0 from i_{edit} based on ϵ_{θ}
- 5: **for** $i = 1, 2, \dots, N$ **do**
- 6: **for** $t = T, T - 1 \dots, 0$ **do**
- 7: **if** $t > t_{\text{zip}}$ **then**
- 8: $x_{t-1} = \sqrt{\alpha_{t-1}}P_t(\tilde{\epsilon}_{\theta}(x_t, t)) + D_t(\epsilon_{\theta}(x_t, t)) + \sigma_t\epsilon_t$. ▷ Editing for i_{edit}
- 9: **else**
- 10: $x_{t-1} = \sqrt{\alpha_{t-1}}P_t(\epsilon_{\theta}(x_t, t)) + D_t(\epsilon_{\theta}(x_t, t)) + \sigma_t\epsilon_t$. ▷ Improve editing quality
- 11: $i_{\text{out}} \leftarrow x_0$
- 12: Update the parameters of Attribute Encoder E_A as Equation 6
- 13: **return** i_{out}

The modified \tilde{P}_t and the original P_t correspond respectively to the formulations presented in Equation 5 and Equation 4. Here, t_{source} and t_{target} reference the text prompts outlined in Appendix B. The latter expression pertains to the reconstruction loss, which takes the form of the L_1 Loss between the generated image and the original image. This reconstruction loss effectively preserves the original features, thereby averting drastic alterations. To balance the aforementioned losses, the hyperparameters λ_{clip} and λ_{recon} are introduced.

During the training phase, the reference image i_{ref} and the editing image i_{edit} are subject to encoding by the Attribute Encoder and Editing Generator, in accordance with the architecture depicted in Figure 2. Consequently, these encoded representations manifest as Δh and h in the latent space, respectively.

The resulting output image i_{out} , generated by a *frozen* diffusion model (Editing Generator) with input $\Delta h + h$, is harnessed for computing the CLIP loss, thereby facilitating the training of the Attribute Encoder. In this process, updates are exclusively applied to the parameters of the Attribute Encoder, while the other components, including the Editing Generator, remain *frozen*.

4.3 IMAGE EDITING VIA ZIP

Given an image $i_{\text{edit}} \in \mathbb{R}^{m \times n}$ and an attribute t_{attr} , the visual features from reference image are integrated into the latent space of i_{edit} in diffusion model as Equation 5, and the textual prompt is used to optimize the Attribute Encoder as Equation 6. We provide an illustration of our framework in Figure 2, and pseudocode in Algorithm 1.

We depict the attribute editing process for the attribute “glasses” facilitated by ZIP in Figure 4. The accompanying noise maps are showcased. As the temporal step t progresses, the cumulative noise across 25 steps is visualized within the noise image. Each noise image is derived from a linear extraction throughout the entire generation process. Concurrently, the respective generated images are displayed. Up until $t = 600$, no Δh is incorporated into the generation, thereby retaining the original image’s style. After reaching the $t = 300$ mark, an additional point to note is that, in order to enhance the quality of the generation process, Δh is still not introduced.

Figure 4 effectively demonstrates that pixels are more *concentrated* on attribute features. This implies the reference image’s efficacy in generating visual components associated with the target attribute. Moreover, in our ZIP process, attribute generation becomes feasible following the insertion of Δh .

5 EXPERIMENTS

Within this section, we present empirical evidence to substantiate the effectiveness of our Zero-shot Inversion Process (ZIP) in conducting semantic latent editing across diverse attributes and

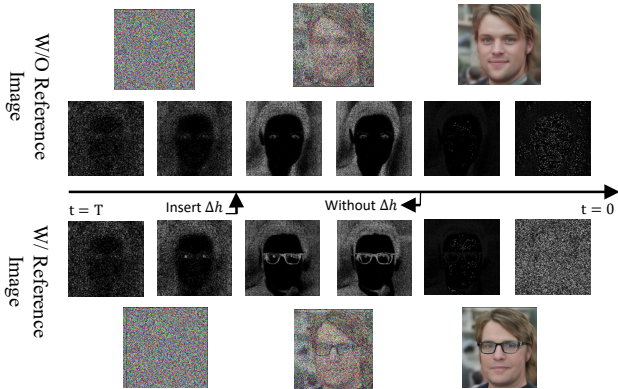


Figure 4: The visualization of noises in ZIP at different time steps t . The image is edited for the attribute of “glasses.” The top half is the editing process without the reference image while the bottom has the reference image. Pixels are more *concentrated* on the features of the attribute, which implies that the reference image effectively works on generating visual items of the target attribute.

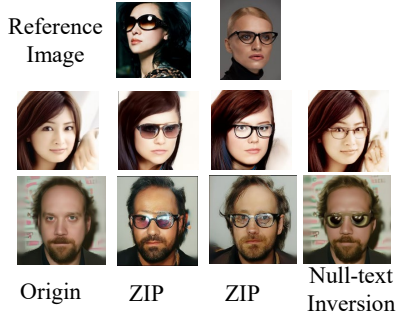


Figure 5: **Consistent Editing:** After specifying an image as reference image, ZIP can make a consistent and controllable editing to the original image. However, other methods, like Null-text Inversion, cannot generate specific style of the attribute.

datasets. Section 5.1 shows the consistent editing of ZIP, where the editing results are consistent with corresponding reference images. Section 5.2, features comparative experiments that underscore ZIP’s superior capabilities in semantic editing. This is observed across both in-domain and out-of-domain attributes. Additionally, the subsequent section, Section 5.3 delves into the outcomes achieved across various datasets.

Baselines. To facilitate comparison, we implement the ILVR (Choi et al., 2021) and Asyrp (Kwon et al., 2022), as benchmarks against ZIP. ILVR operates as an image-guided approach to semantic synthesis. In the forthcoming experiments, ILVR’s parameters include a low-pass filter scale of $N = 64$ and a time step of $t = 100$. Asyrp, on the other hand, ascertains that diffusion models inherently possess a semantic latent space, rendering it a state-of-the-art text-guided approach. For our Asyrp implementation, we adhere to the default parameters stipulated in the official codebase.

Implement Details. All methods, including ZIP, are subjected to training on the CelebA-HQ (Karras et al., 2018), LSUN-church, and LSUN-bedroom datasets (Yu et al., 2015). In the case of ZIP, the Edit Generator draws upon DDPM++ (Song et al., 2020b), and the employed model is sourced from the official pre-trained checkpoint, thus bypassing any training specific to our experiments. Our Visual Generator is realized through Unidiffuser (Bao et al., 2023), while the Text Encoder is represented by the CLIP model (Radford et al., 2021), both using the official checkpoints. Of note, only the last five layers of the Attribute Encoder are subject to training within the ZIP framework. Further details can be explored in the supplementary materials provided.

Evaluation. To assess the proficiency of image generation and editing, prior research has introduced numerous evaluation metrics. In this study, we opt to employ the Inception Score (ISC) (Salimans et al., 2016) and the Fréchet Inception Distance (FID) (Szegedy et al., 2016) as indicators of the image generation quality. Furthermore, the CLIP Score (Radford et al., 2021) is leveraged to gauge the alignment between edited images and their intended semantic targets.

5.1 CONSISTENCE OF ZIP

Our ZIP shows high consistence with the reference images. Though the previous works, such as Prompt2Prompt (Hertz et al., 2022) and Null-Text Inversion (Mokady et al., 2022), makes a realistic editing for real images, it is still challenging to control the style of attributes. As shown in Figure 5, with a specific reference image, ZIP generates the same styles of glasses for different images. However, Null-Text Inversion can only generate the glasses, which cannot be controlled.

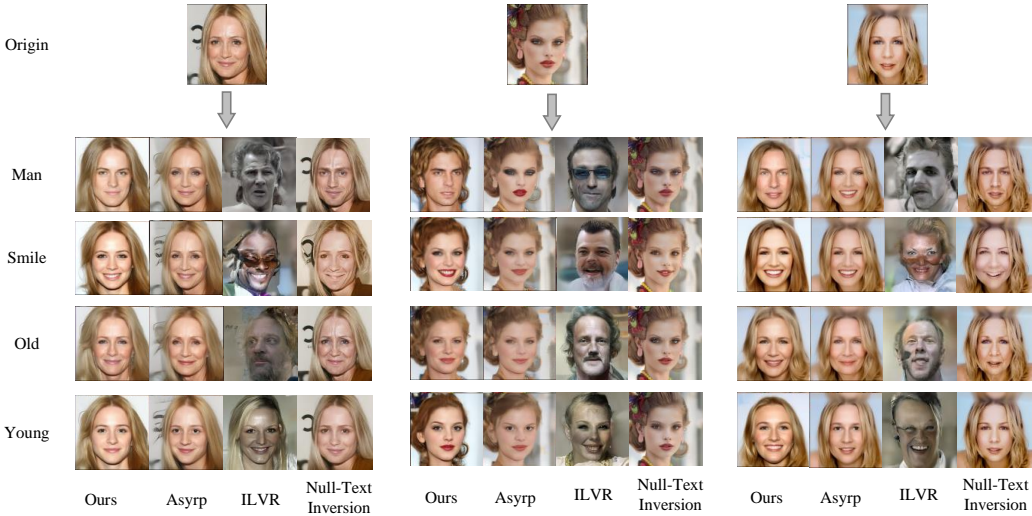


Figure 6: **Editing results for in-domain attributes.** The same attributes are modified by ZIP, Asyrp and ILVR.

Table 1: In-domain Attributes Modification

Method	Man			Old			Smiling			Young		
	ISC	FID	CLIP	ISC	FID	CLIP	ISC	FID	CLIP	ISC	FID	CLIP
ILVR (Choi et al., 2021)	2.623	150.2	22.24	2.361	145.1	23.26	2.557	223.7	25.59	2.582	147.9	22.70
Asyrp (Kwon et al., 2022)	1.808	77.65	19.15	1.833	77.82	22.73	1.760	73.93	<u>26.31</u>	1.705	80.03	26.11
Null-text Inversion (Mokady et al., 2022)	2.219	52.23	<u>23.02</u>	2.075	50.65	22.46	2.014	44.25	25.98	2.089	40.52	24.42
Ours	1.592	87.31	22.38	1.778	85.96	<u>22.79</u>	1.573	85.36	27.01	1.624	85.28	<u>25.07</u>

5.2 GENERALIZATION OF ZIP

In our evaluation, ZIP is assessed from two perspectives of generalization. Firstly, we scrutinize its performance in manipulating attributes that are inherently present within the datasets. For instance, in CelebA-HQ, numerous images feature individuals with smiling expressions, and the attribute of “smiling” is explicitly labeled in the datasets. For the purposes of this evaluation, we refer to these attributes as “In-domain Attributes”. Conversely, we examine attributes that are not explicitly represented in the datasets, such as “Add glasses”. These are referred to as “Out-of-domain Attributes”.

Figure 6 presents the outcomes of our method concerning in-domain attributes, juxtaposed with results from ILVR and Asyrp. Our approach successfully alters specific attributes while keeping other attributes constant. This includes modifying expressions of individuals. In the context of text-guided approaches like Asyrp, attributes that don’t necessitate alterations in visual features are handled adeptly. For example, attributes like “smiling” which entail facial feature deformations, can be effectively edited by Asyrp. However, altering attributes like gender demands replacing female features with male features, a feat that cannot be accomplished solely through text-guided methods. Meanwhile, for image-guided approaches such as ILVR, the relationship between the target attribute and the reference image can be less defined. Consequently, ILVR is prone to producing distorted or inaccurately manipulated images, as depicted in Figure 6. ZIP’s strength lies in its capacity to synergize textual prompts with reference images to yield high-quality edits across a diverse array of attributes. The outcomes displayed in Table 1 corroborate this, demonstrating that ZIP achieves superior editing outcomes for attributes, without compromising on quality, when compared to alternative methods.

Figure 7 portrays the outcomes pertaining to out-of-domain attributes, such as the addition of glasses and alteration of makeup. ZIP consistently achieves the highest CLIP scores across all attributes, a fact corroborated by the data presented in Table 2 and 3. As observed with in-domain attributes, Asyrp’s performance is impeded by its inability to access additional visual features. Conversely, ZIP demonstrates its competence in generating novel attributes by leveraging the capabilities of the

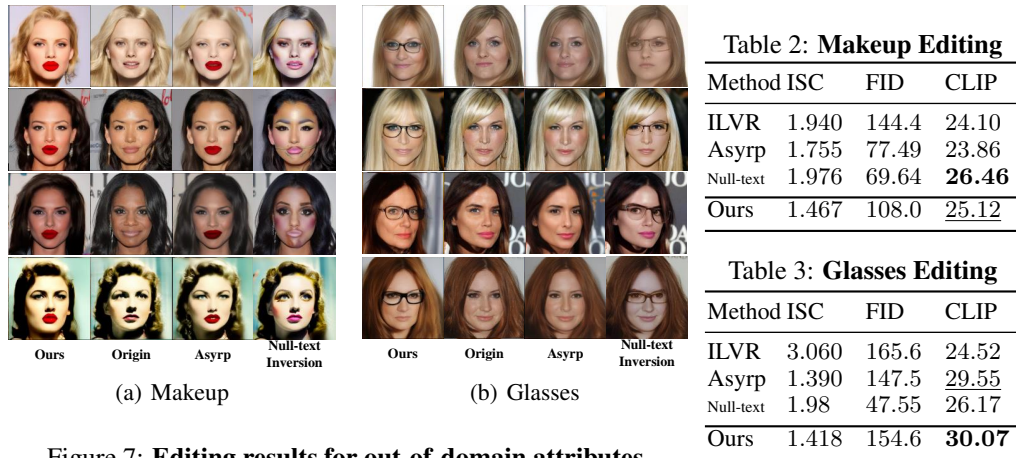


Figure 7: Editing results for out-of-domain attributes.



Figure 8: Editing results of ZIP on various datasets. We conduct experiments on CelebA-HQ, LSUN-church and LSUN-bedroom.

Visual Generator and Text Encoder. This facilitates the generalization of both visual and semantic information, rendering ZIP highly proficient in addressing out-of-domain attributes.

5.3 MORE RESULTS

Figure 8 illustrates the visual outcomes attained through our methodology across diverse datasets. ZIP demonstrates its capacity to synthesize attributes present within the training datasets, such as age and gender in CelebA-HQ. Additionally, it can manipulate attributes based on the semantics provided by the text prompt, exemplified by “gothic” in LSUN-church. This versatility in semantic synthesis showcases ZIP’s ability to accomplish varied tasks solely through training with distinct text prompts.

6 CONCLUSION

This paper introduces ZIP, a novel approach for the manipulation of real-world images using natural language. ZIP achieves this by infusing a blend of generated visual reference and textual guidance

into the semantic latent space of a *frozen* diffusion model. By bridging the gap between visual patterns and textual semantics, ZIP is capable of effectively altering attributes, irrespective of whether they are in-domain or out-of-domain. In the future, our research will delve into enhancing the accuracy of attribute acquisition from reference images. This involves refining methods for specifying attributes with similar visual features, thus further improving the manipulation process.

Limitation. Indeed, while ZIP excels in producing realistic edits for real images, it’s important to acknowledge that it faces a limitation in the absence of a target mask, similar to the capability demonstrated by Imagen Editor (Wang et al., 2022). Imagen Editor’s ability to use an editing mask as input allows it to achieve intensive and precise editing of the target attributes. On the other hand, ZIP’s operation without a clearly defined mask might lead to inadvertent alignment of visual features and text prompts, potentially resulting in incorrect or unintended modifications. This points to an avenue for improvement in the future, as addressing this limitation could further enhance ZIP’s editing accuracy.

Acknowledgements. R. C. Qiu would like to acknowledge the National Natural Science Foundation of China (via fund NSFC-12141107), the Key Research and Development Program of Hubei (2021BAA037) and of Guangxi (GuiKe-AB21196034).

REFERENCES

- Avrahami, O., Lischinski, D., and Fried, O. (2022). Blended diffusion for text-driven editing of natural images. In *CVPR*, pages 18208–18218.
- Bao, F., Nie, S., Xue, K., Li, C., Pu, S., Wang, Y., Yue, G., Cao, Y., Su, H., and Zhu, J. (2023). One transformer fits all distributions in multi-modal diffusion at scale. *arXiv preprint arXiv:2303.06555*.
- Brooks, T., Holynski, A., and Efros, A. A. (2023). Instructpix2pix: Learning to follow image editing instructions. In *CVPR*.
- Brown, T., Mann, B., Ryder, N., Subbiah, M., Kaplan, J. D., Dhariwal, P., Neelakantan, A., Shyam, P., Sastry, G., Askell, A., et al. (2020). Language models are few-shot learners. *Advances in neural information processing systems*, 33:1877–1901.
- Choi, J., Kim, S., Jeong, Y., Gwon, Y., and Yoon, S. (2021). Ilvr: Conditioning method for denoising diffusion probabilistic models. *arXiv preprint arXiv:2108.02938*.
- Daras, G. and Dimakis, A. G. (2022). Multiresolution textual inversion. *arXiv preprint arXiv:2211.17115*.
- Elarabawy, A., Kamath, H., and Denton, S. (2022). Direct inversion: Optimization-free text-driven real image editing with diffusion models. *arXiv preprint arXiv:2211.07825*.
- Gal, R., Patashnik, O., Maron, H., Bermano, A. H., Chechik, G., and Cohen-Or, D. (2022). Stylegan-nada: Clip-guided domain adaptation of image generators. *ACM Transactions on Graphics (TOG)*, 41(4):1–13.
- Google (2023). Palm 2 technical report.
- Hertz, A., Mokady, R., Tenenbaum, J., Aberman, K., Pritch, Y., and Cohen-Or, D. (2022). Prompt-to-prompt image editing with cross attention control. *arXiv preprint arXiv:2208.01626*.
- Heusel, M., Ramsauer, H., Unterthiner, T., Nessler, B., and Hochreiter, S. (2017a). Gans trained by a two time-scale update rule converge to a local nash equilibrium. *Advances in neural information processing systems*, 30.
- Heusel, M., Ramsauer, H., Unterthiner, T., Nessler, B., and Hochreiter, S. (2017b). Gans trained by a two time-scale update rule converge to a local nash equilibrium. *Advances in neural information processing systems*, 30.
- Ho, J., Jain, A., and Abbeel, P. (2020). Denoising diffusion probabilistic models. *Advances in Neural Information Processing Systems*, 33:6840–6851.

- Jia, X., Zhao, Y., Chan, K. C., Li, Y., Zhang, H., Gong, B., Hou, T., Wang, H., and Su, Y.-C. (2023). Taming encoder for zero fine-tuning image customization with text-to-image diffusion models. *arXiv preprint arXiv:2304.02642*.
- Karras, T., Aila, T., Laine, S., and Lehtinen, J. (2018). Progressive growing of gans for improved quality, stability, and variation. In *International Conference on Learning Representations*.
- Karras, T., Laine, S., Aittala, M., Hellsten, J., Lehtinen, J., and Aila, T. (2020). Analyzing and improving the image quality of stylegan. In *Proceedings of the IEEE/CVF conference on computer vision and pattern recognition*, pages 8110–8119.
- Kim, G., Kwon, T., and Ye, J. C. (2022). Diffusionclip: Text-guided diffusion models for robust image manipulation. In *Proceedings of the IEEE/CVF Conference on Computer Vision and Pattern Recognition*, pages 2426–2435.
- Kwon, M., Jeong, J., and Uh, Y. (2022). Diffusion models already have a semantic latent space. *arXiv preprint arXiv:2210.10960*.
- Lugmayr, A., Danelljan, M., Romero, A., Yu, F., Timofte, R., and Van Gool, L. (2022). Repaint: Inpainting using denoising diffusion probabilistic models. In *Proceedings of the IEEE/CVF Conference on Computer Vision and Pattern Recognition*, pages 11461–11471.
- Meng, C., He, Y., Song, Y., Song, J., Wu, J., Zhu, J.-Y., and Ermon, S. (2021). Sdedit: Guided image synthesis and editing with stochastic differential equations. In *International Conference on Learning Representations*.
- Mokady, R., Hertz, A., Aberman, K., Pritch, Y., and Cohen-Or, D. (2022). Null-text inversion for editing real images using guided diffusion models. *arXiv preprint arXiv:2211.09794*.
- Nguyen, T., Li, Y., Ojha, U., and Lee, Y. J. (2023). Visual instruction inversion: Image editing via visual prompting. *arXiv preprint arXiv:2307.14331*.
- Nitzan, Y., Aberman, K., He, Q., Liba, O., Yarom, M., Gandelsman, Y., Mosseri, I., Pritch, Y., and Cohen-Or, D. (2022). Mystyle: A personalized generative prior. *ACM Transactions on Graphics (TOG)*, 41(6):1–10.
- OpenAI (2023). Gpt-4 technical report.
- Radford, A., Kim, J. W., Hallacy, C., Ramesh, A., Goh, G., Agarwal, S., Sastry, G., Askell, A., Mishkin, P., Clark, J., et al. (2021). Learning transferable visual models from natural language supervision. In *International conference on machine learning*, pages 8748–8763. PMLR.
- Ramesh, A., Pavlov, M., Goh, G., Gray, S., Voss, C., Radford, A., Chen, M., and Sutskever, I. (2021). Zero-shot text-to-image generation. In *International Conference on Machine Learning*, pages 8821–8831. PMLR.
- Rombach, R., Blattmann, A., Lorenz, D., Esser, P., and Ommer, B. (2022). High-resolution image synthesis with latent diffusion models. In *Proceedings of the IEEE/CVF Conference on Computer Vision and Pattern Recognition*, pages 10684–10695.
- Ronneberger, O., Fischer, P., and Brox, T. (2015). U-net: Convolutional networks for biomedical image segmentation. In *Medical Image Computing and Computer-Assisted Intervention—MICCAI 2015: 18th International Conference, Munich, Germany, October 5-9, 2015, Proceedings, Part III 18*, pages 234–241. Springer.
- Saharia, C., Chan, W., Saxena, S., Li, L., Whang, J., Denton, E. L., Ghasemipour, K., Gontijo Lopes, R., Karagol Ayan, B., Salimans, T., et al. (2022). Photorealistic text-to-image diffusion models with deep language understanding. *Advances in Neural Information Processing Systems*, 35:36479–36494.
- Salimans, T., Goodfellow, I., Zaremba, W., Cheung, V., Radford, A., and Chen, X. (2016). Improved techniques for training gans. *Advances in neural information processing systems*, 29.

- Schick, T. and Schütze, H. (2020). Exploiting cloze questions for few shot text classification and natural language inference. *arXiv preprint arXiv:2001.07676*.
- Song, J., Meng, C., and Ermon, S. (2020a). Denoising diffusion implicit models. *arXiv preprint arXiv:2010.02502*.
- Song, Y., Sohl-Dickstein, J., Kingma, D. P., Kumar, A., Ermon, S., and Poole, B. (2020b). Score-based generative modeling through stochastic differential equations. *arXiv preprint arXiv:2011.13456*.
- Szegedy, C., Vanhoucke, V., Ioffe, S., Shlens, J., and Wojna, Z. (2016). Rethinking the inception architecture for computer vision. In *Proceedings of the IEEE conference on computer vision and pattern recognition*, pages 2818–2826.
- Wallace, B., Gokul, A., and Naik, N. (2022). Edict: Exact diffusion inversion via coupled transformations. *arXiv preprint arXiv:2211.12446*.
- Wang, S., Saharia, C., Montgomery, C., Pont-Tuset, J., Noy, S., Pellegrini, S., Onoe, Y., Laszlo, S., Fleet, D. J., Soricut, R., et al. (2022). Imagen editor and editbench: Advancing and evaluating text-guided image inpainting. *arXiv preprint arXiv:2212.06909*.
- Yu, F., Seff, A., Zhang, Y., Song, S., Funkhouser, T., and Xiao, J. (2015). Lsun: Construction of a large-scale image dataset using deep learning with humans in the loop. *arXiv preprint arXiv:1506.03365*.

Supplementary Material

Zero-shot Inversion Process for Image Attribute Editing with Diffusion Models

A USEFUL LEMMAS

Theorem 1 (Kwon et al. (2022, Theorem 1)). *Let ϵ_t^θ be a predicted noise during the original reverse process at t and $\tilde{\epsilon}_t^\theta$ be its shifted counterpart. Then, $\tilde{x}_{t-1} \approx x_{t-1}$ where $\tilde{x}_{t-1} = \sqrt{\alpha_{t-1}}P_t(\tilde{\epsilon}_t^\theta(x_t)) + D_t(\tilde{\epsilon}_t^\theta(x_t))$. I.e., the shifted terms of $\tilde{\epsilon}_t^\theta$ in P_t and D_t destruct each other in the reverse process.*

B DETAIL OF OUR FRAMEWORK

Text Encoder: To extract textual features, the text prompt t derived from the attribute t_{attr} is encoded into a vector. This vector is subsequently utilized to calculate the CLIP loss in tandem with the target image. As exemplified by the work of Brown et al. (2020), the evolution of substantial language models has significantly drawn attention to the text prompt, especially in the realm of multimodal applications, e.g., GPT-4 (OpenAI, 2023) and PaLM2 (Google, 2023). These language models have been extensively trained on a vast array of linguistic data and have proven to be adept in few-shot learning scenarios. In this study, the CLIP model (Radford et al., 2021) is employed as the Text Encoder.

In our work, the text prompt t contains two components: t_{source} and t_{target} . These components are generated through the following procedure. Let E_T denote the text encoder equipped with vocabulary V . The attribute t_{attr} constitutes a sequence of phrases denoted as $t_{\text{attr}} = (s_1, \dots, s_k)$, where each $s_i \in V$. To illustrate with an example, when the attribute t_{attr} is “glasses,” the value of k is 1. Drawing parallels with prompts in natural language processing (NLP) (Schick and Schütze, 2020), we establish the notion of a pattern as a function P , which takes the attribute t_{attr} as input and generates two phrases or sentences, t_{source} and t_{target} , in the vocabulary V . This dynamic yields the text prompt $t = (t_{\text{source}}, t_{\text{target}})$.

For instance, when the attribute t_{attr} pertains to a person, a conceivable pattern could be $P(t_{\text{attr}}) = (\text{“a person”}, \text{“a person with } t_{\text{attr}}\text{”})$. Consequently, if the input attribute is $t_{\text{attr}} = \text{“glasses”}$, the derived text prompt would be $P(t_{\text{attr}}) = (\text{“a person”}, \text{“a person with glasses”})$, from which $t_{\text{source}} = \text{“a person”}$ and $t_{\text{target}} = \text{“a person with glasses.”}$ Collectively, they constitute the comprehensive text prompt t . After that, the Text Encoder processes this prompt to encode t_{source} as $E_T(t_{\text{source}}) \in \mathbb{R}^d$ and t_{target} as $E_T(t_{\text{target}}) \in \mathbb{R}^d$.

Visual Generator: To acquire the visual attributes corresponding to the specified attribute, we employ a text-image model known as the Visual Generator. Notably, large scale generative models have demonstrated pronounced robustness and adaptability in conditional generation tasks (Saharia et al., 2022; Rombach et al., 2022). While these models may not possess the capacity to pinpoint or precisely modify attributes, they are proficient in generating attribute-associated features within the visual domain. In this study, we adopt UniDiffuser (Bao et al., 2023) as the designated Visual Generator. UniDiffuser uniquely combines text and image generation within a single model, leveraging the concurrent utilization of marginal, conditional, and joint distributions derived from multimodal data.

To acquire the reference image, denoted as $i_{\text{ref}} = G_V(t_{\text{target}})$, images are extracted from the conditional distribution $p(x_0|t_{\text{target}})$ through the following process:

$$p_\theta(x_0|t_{\text{target}}) = \int p_\theta(x_{0:T}|t_{\text{target}})dx_{1:T}, p_\theta(x_{0:T}|t_{\text{target}}) = p(x_T) \prod_{t=1}^T p_\theta(x_{t-1}|x_t, t_{\text{target}}) \quad (7)$$

where $x_T \sim \mathcal{N}(0, \mathbf{I})$, $p_\theta(x_{t-1}|x_t, t_{\text{target}}) = \mathcal{N}(x_{t-1}|\mu_t(x_t, t_{\text{target}}), \sigma_t^2 \mathbf{I})$, and the mean $\mu_t = \frac{1}{\sqrt{\alpha_t}}(x_t - \frac{\beta_t}{\sqrt{1-\alpha_t}}\mathbb{E}[\epsilon^x|x_t, t_{\text{target}}])$ is predicted by a noise predictor ϵ_θ (Bao et al., 2023). Upon completion of the denoising procedure, we obtain the reference image i_{ref} .

Attribute Encoder: The Attribute Encoder E_A functions as a downsampling network, encompassing attention blocks and residual blocks. This type of downsampling network has found wide application in both detection (Ronneberger et al., 2015) and generation (Ho et al., 2020). Through down-sampling, the original image undergoes encoding into a latent space, thereby resulting in a transformed representation. Upon input of the reference image, the Attribute Encoder yields the latent embedding of visual features, i.e., $E_A(i_{\text{ref}}) \in \mathbb{R}^D$. This embedding, represented by $E_A(i_{\text{ref}})$, efficiently facilitates attribute manipulation.

Edit Generator: The role of the Edit Generator revolves around the generation of the target image. The efficacy of diffusion models has been extensively showcased in prior research (Ho et al., 2020; Choi et al., 2021). In this study, the DDIM model (Song et al., 2020a) is harnessed to generate images, as defined by Equation 2.

C EXPERIMENT DETAILS

C.1 PARAMETERS

The parameters of our ZIP in different datasets are shown in Table 4. The code is also attached to the supplementary materials.

Table 4: The parameters of ZIP

Parameter	CelebA-HQ	LSUN-church	LSUN-bedroom
Resolution of images	256×256	256×256	256×256
Time step T	1000	1000	1000
Batch size of training	9	9	9
Inversion time step	40	40	40
Learning rate of training	0.5	0.5	0.5
The weight of visual features Δh	0.3	0.1	0.1
The weight of CLIP loss λ_{clip}	0.8	2	0.8
The weight of reconstruction loss λ_{recon}	3	3	3

C.2 EVALUATION

Inception Score: Inception Score (ISC) (Salimans et al., 2016) is used to assess how realistic generated images are. The computation of ISC is:

$$ISC = \exp(\mathbb{E}_x KL(p(y|x)||p(y))) \quad (8)$$

where $KL(p(y|x)||p(y))$ is the KL divergence between the conditional distribution $p(y|x)$ and the marginal distribution $p(y)$. Both the conditional and marginal distribution is calculated from features extracted from the images. The score is calculated on random splits of the images such that both a mean and standard deviation of the score are returned. In this paper, ISC is computed based on the original weights from (Heusel et al., 2017a).

Fréchet Inception Distance: Fréchet Inception Distance (FID) (Szegedy et al., 2016) also is used to assess the quality of generated images. Different from ISC, which is computed only by the generation images ignoring the real images, FID uses the features from Inception Network to evaluate the similarity of real images and generated images. FID is computed by:

$$FID = \|\mu - \mu_\omega\| + \text{tr}(\Sigma + \Sigma_\omega - 2(\Sigma\Sigma_\omega)^{\frac{1}{2}}) \quad (9)$$

where $\mathcal{N}(\mu, \Sigma)$ is the multivariate normal distribution estimated from Inception v3 (Szegedy et al., 2016) features calculated on real life images and $\mathcal{N}(\mu_\omega, \Sigma_\omega)$ is the multivariate normal distribution

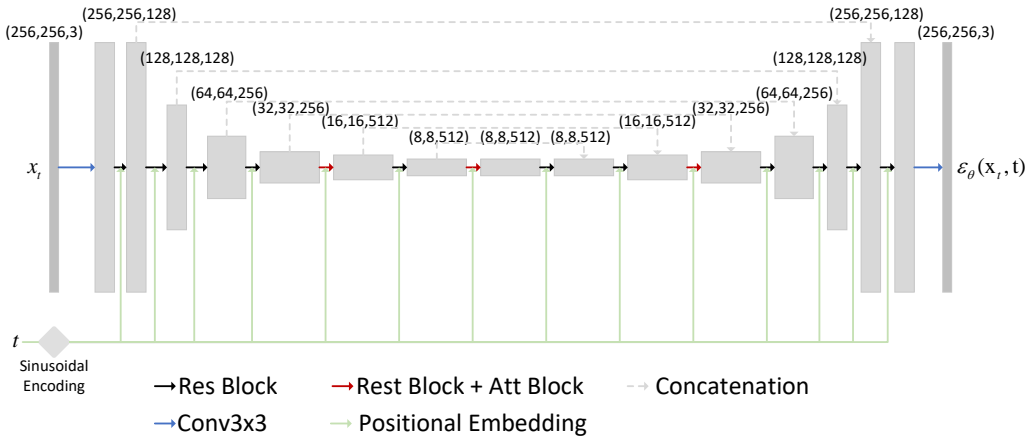


Figure 9: **The Architecture of Editing Generator.** The U-Net architecture of Editing Generator outputs 256×256 images. The Δh is inserted into the middle layer.

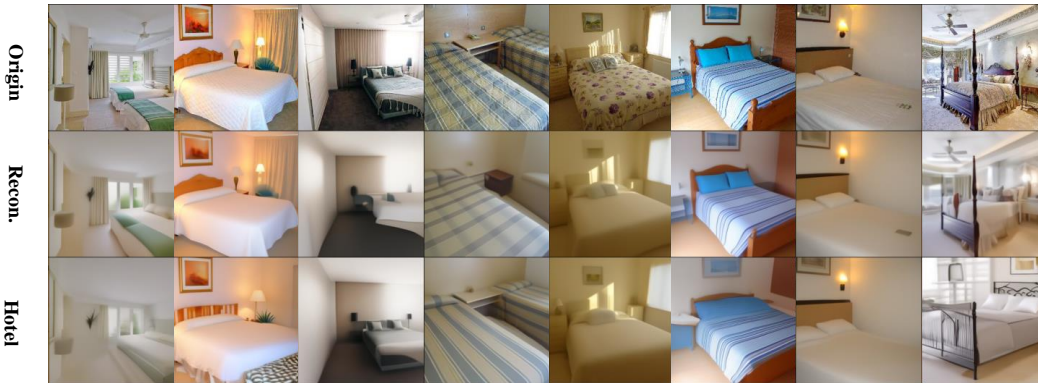


Figure 10: **The results in LSUN-bedroom.**

estimated from Inception v3 features calculated on generated images. In this paper, FID is computed based on the original weights from (Heusel et al., 2017b).

CLIP Score: CLIP Score (Radford et al., 2021) is a reference-free metric that can be used to evaluate the correlation between a generated caption for an image and the actual content of the image. It has been found to be highly correlated with human judgment. The metric is defined as:

$$extCLIPScore(i, c) = \max(100 * \cos(E_i, E_c), 0) \tag{10}$$

which corresponds to the cosine similarity between visual CLIP embedding E_i for an image i and textual CLIP embedding E_c for an caption c . In the following experiments, the model "clip-vit-base-patch16" from official checkpoints of CLIP model (Radford et al., 2021) is used to evaluate the attribute changes.

In our experiments, we use the code of torch-fidelity[†] to compute ISC and FID. CLIP Score is computed based on TorchMetrics[‡].

[†] <https://github.com/toshas/torch-fidelity>.
[‡] https://torchmetrics.readthedocs.io/en/stable/multimodal/clip_score.html.

Table 5: The results of LSUN dataset

Method	gothic			night			department			factory			bedroom-hotel		
	ISC	FID	CLIP	ISC	FID	CLIP	ISC	FID	CLIP	ISC	FID	CLIP	ISC	FID	CLIP
Asyrp (Kwon et al., 2022)	2.769	93.13	21.98	3.198	111.4	22.05	3.290	118.3	23.49	3.175	109.7	22.15	2.033	102.5	24.64
Ours	2.958	118.0	24.24	3.486	209.9	23.24	2.631	112.0	23.21	3.346	133.7	22.92	2.599	115.5	26.52

D NETWORK ARCHITECTURE

D.1 ATTRIBUTE ENCODER AND EDITING GENERATOR

We use a U-net backbone as our Editing Generator as shown in Figure 9. The Attribute Encoder shares parameters with the Editing Generator in the down-sampling parts (the first eight layers). In the training process, we only update the parameters of the Attribute Encoder.

D.2 OTHERS

The other parts of our framework are frozen with the official checkpoints. We use Unidiffuser (Bao et al., 2023) and CLIP model (Radford et al., 2021) as the Visual Generator and the Text Encoder with the official checkpoints, respectively.

E MORE RESULTS

We supply more results for different datasets, such as LSUN-church in Figure 11 LSUN-bedroom in Figure 10, and CelebA-HQ in in Figure 15. The other attributes for different datasets, such as “Department” and “Factory”, are shown in a bigger size.

In Figure 12 and Figure 13, we show more results in test data for the in-domain attribute “gender” and “smile”. For visual features, ZIP can generate extra features of gender. For the deformation of facial features, ZIP can also change the original features well. Moreover, in Figure 14, the out-of-domain attribute is shown.

Also, as Figure 16 shows, the top half is the editing process for the attribute “makeup” without the reference image while the bottom has the reference image. Though both of them generate the details of the face, the results with the reference image are more *concentrated* on the features of the attribute “makeup”, such as the part of lips.



Figure 11: The results in LSUN-church.



Figure 12: The results in CelebA-HQ for the attribute “gender”.



Figure 13: The results in CelebA-HQ for the attribute “smile”.



Figure 14: The results in CelebA-HQ for the attribute “makeup”.



Figure 15: The results in CelebA-HQ.

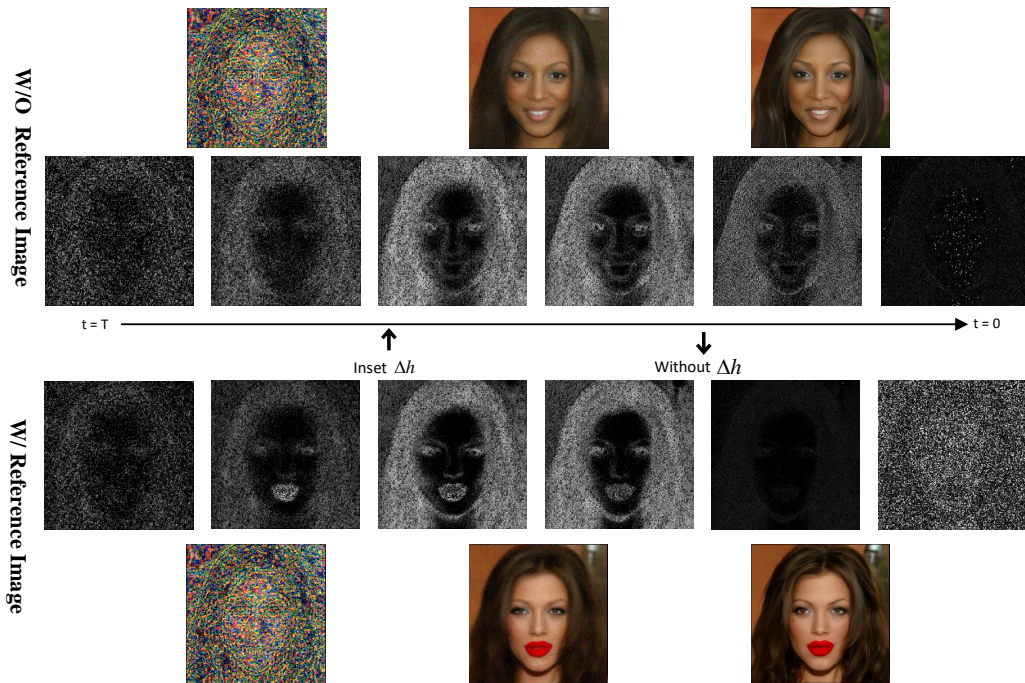


Figure 16: The visualization of noises in ZIP at different time steps t . The image is edited for the attribute of “makeup.”